ISBN: 978-3-95450-262-2 ISSN: 2673-5350 doi: 10.18429/JACoW-IBIC2025-TUPCO22

CHERENKOV RADIATION SPECTRAL AND RESOLUTION PROPERTIES STUDIES AT SINBAD ARES

A. Novokshonov*, G. Kube, W. Kuropka, B. Stacey, M. Kellermeier, T. Vinatier
Deutsches Elektronen-Synchrotron (DESY), Hamburg, Germany
A. P. Potylitsyn, Institute of Applied Problems of Physics of the National Academy of Sciences of the Republic of Armenia (IAPP NAS RA), Erevan, Armenia

Abstract

Optical Cherenkov Radiation (ChR) is a well-known type of radiation, which is utilized in different fields of physics such as charged particle detection or generation of intense THz radiation. It is also widely used in beam diagnostics, for instance, in beam loss monitors or for bunch length measurements. In addition, it is of potential interest for transverse beam profile diagnostics as an alternative for standard techniques as scintillating screens and optical transition radiation. In this work, spectral and resolution properties of optical ChR were studied at the SINBAD ARES accelerator with an electron beam energy of 150 MeV. Several fused silica crystals of different thicknesses were used as radiators. They could be rotated relative to the beam, which allowed to investigate the angular dependency of the ChR spectrum which is quasi-monochromatic. The monochromatization effect arises from the frequency-dependent nature of the fused silica permittivity. In addition, the beam size dependency on the target angle was investigated in view of differences for various crystal thicknesses.

INTRODUCTION

Cherenkov radiation (ChR) [1,2] is widely used across various fields of physics, including the design and construction of detectors [3], beam diagnostics in modern accelerators [4], and as a radiation source [5]. ChR exhibits three main characteristics: directional emission, a velocity threshold for particle excitation, and a continuous spectrum extending from approximately 100 nm to centimeter wavelengths. The first of these features, directional emission, is described by the following formula:

$$\theta_{ch} = \arccos\left(\frac{1}{\beta\, n(\lambda)}\right), \tag{1}$$

where $\theta_c h$ is ChR opening angle, $\beta = v/c$ is the reduced velocity of the moving charged particle and $n(\lambda)$ is the wavelength dependent refractive index of the media. Consequently the threshold condition is as follows:

$$\beta\, n(\lambda) > 1. \tag{2}$$

The threshold defines the radiation spectral range for constant particle velocity.

Interest in studying ChR has increased in recent years. Advances in the design of artificial structures have enabled the fabrication of materials with unusual electromagnetic properties such as metamaterials, photonic crystals, and metastructures at the nanoscale. These materials can serve as ChR targets and significantly modify its emission characteristics. In beam diagnostics, ChR is already widely used in beam loss monitors (BLMs), and Cherenkov diffraction radiation (ChDR) can be employed for beam profile monitoring or beam position measurements [6]. Possibly, ChR has the potential to serve as an alternative to standard techniques such as optical transition radiation (OTR) [7] and scintillating screens [8], both of which have inherent limitations.

EXPERIMENTAL SETUP

A series of measurements was carried out using the 150 MeV electron beam of the SINBAD ARES linac. The experimental setup is shown in Fig. 1. Several quartz plates of different thicknesses (0.2, 0.4, 0.6, 1, and 2 mm) were investigated, along with a 0.2 mm thick GAGG:Ce scintillator used as a reference. The samples were placed 60 mm downstream of the accelerator's exit window, which was made of 50 µm thick titanium. Each crystal could be rotated around its vertical axis. Two types of detectors were employed: a CMOS camera and a spectrometer. The camera was a Basler acA2440-20gm equipped with a Schneider-Kreuznach Makro-Symmar 5.6/80 objective, while the spectrometer was a Hamamatsu C10082CA mini-spectrometer. Light was coupled into the spectrometer using a 1 m long Hamamatsu A15262-01 fiber with a 0.6 mm pure quartz core. A MgF_2 lens with a 100 mm focal length collimated the light into the fiber. Both images and spectra were recorded at a 45° observation angle.

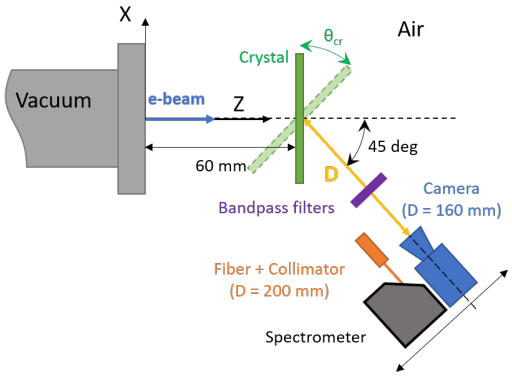

Figure 1: Scheme of the experiment.

* artem.novokshonov@desy.de

ISBN: 978-3-95450-262-2 ISSN: 2673-5350 doi: 10.18429/JACoW-IBIC2025-TUPCO22

Additionally, five different bandpass filters could be inserted: four with central wavelengths at 450, 500, 550, and 600 nm, and one at 550 nm with a 10 nm FWHM. The other three filters had a 40 nm FWHM.

RESULTS

Figure 2 shows a comparison of the measured beam sizes. The upper plot corresponds to the horizontal dimensions, while the lower plot shows the vertical ones. In both cases, the dashed line indicates the bunch size obtained from the GAGG screen, averaged over ten measurements. So the beam size measured by the scintillator was $\sigma_x \times \sigma_y = 324 \times 186$ µm. The bunch charge was 155 pC. No filters were applied in this measurement. Both the ChR and scintillator data represent projection sizes. The results demonstrate that

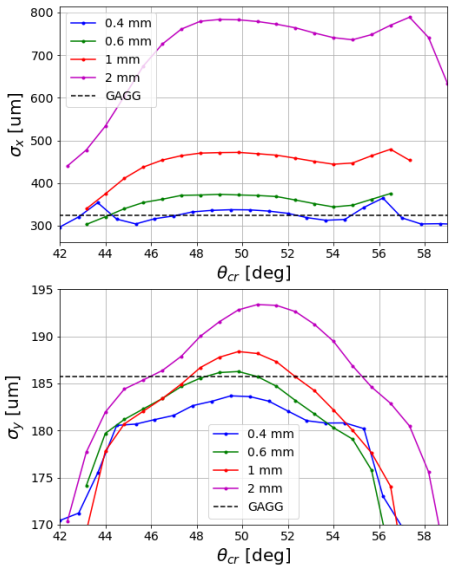

Figure 2: Comparison of sizes with no filter applied: the upper plot - horizontal sizes; the lower one - vertical sizes.

the horizontal beam size increases with crystal thickness. For the 2 mm crystal, the image is already dominated by the point-spread function (PSF). Among the investigated samples, the 0.4 mm crystal provides the closest agreement with the scintillator measurement.

In addition to the overall size trend, two distinct peaks are visible on either side of the 0.4 mm crystal. Similar features appear for the other crystals, although the left peak becomes smeared out at larger thicknesses. For example, there was another measurement with a 0.2 mm crystal at 150 MeV electron energy and a bunch charge of 67 pC (Fig.3) shows the peaks clearly. The beam size in this case was $\sigma_x \times \sigma_y = 212 \times 305$ µm. The origin of these peaks is illustrated in Fig.4. Rotating the crystal alters both the ChR spectrum and the portion of its emission cone captured by the objective. This effect is asymmetric in the horizontal plane, while in the vertical plane no additional peaks are introduced. Notably, the observed peaks align well with the rise and fall of the vertical measurements, supporting this interpretation. However, the effect becomes increasingly smeared as the crystal thickness increases. It is also noticeable that the

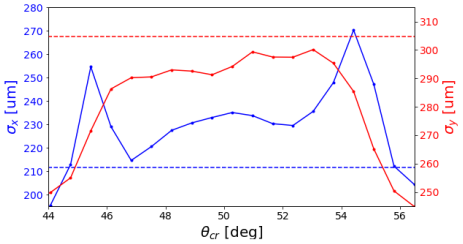

Figure 3: A measurement with 200 µm fused silica crystal at 150 MeV and 67 pC.

ChR vertical sizes are systematically smaller. In Fig. 2, the results for the 0.4 mm crystal show that the vertical size remains below the scintillator value, while the horizontal size is comparable.

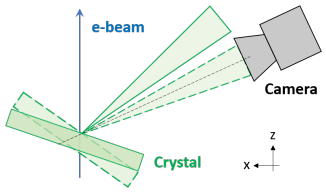

Figure 4: Origin of the horizontal size variations along the scans.

Subsequent measurements were performed with the bandpass filters inserted. The results for the 0.6 mm crystal are presented in Fig. 5, where the upper plot shows the horizontal sizes and the lower plot the vertical ones. In the horizontal direction, almost no difference is observed, although the "no filter" case yields the largest values. In contrast, the vertical direction exhibits a clearer dependence on wavelength, with the "no filter" case again giving the highest result. The results for the 2 mm thick crystal are shown in Fig. 6. In this case, the horizontal sizes exhibit even smaller differences between filters, although the overall size is larger, consistent with the images being dominated by the PSF for this crystal thickness. In the vertical direction, the differences between measurements with and without filters are more pronounced, yet remain relatively small (approximately 4 %). A more insightful comparison could be obtained for smaller beam sizes, which was not feasible in these measurements due to the beam being in air. The crystal thinner than 0.6 mm reveal even less affect, and the 1 mm thick crystal shows an affect in-between. Therefore both cases are not worth showing them here.

The final part of the study involved spectral measurements. Angle scans were performed from 47° to 59° in 1° steps. Three representative spectra are shown in Fig. 7. For the 2 mm thick crystal, the maximum peak intensity occurs at 55°. In contrast, the 0.6 and 1 mm crystals exhibit their

ISBN: 978-3-95450-262-2 ISSN: 2673-5350 doi: 10.18429/JACoW-IBIC2025-TUPCO22

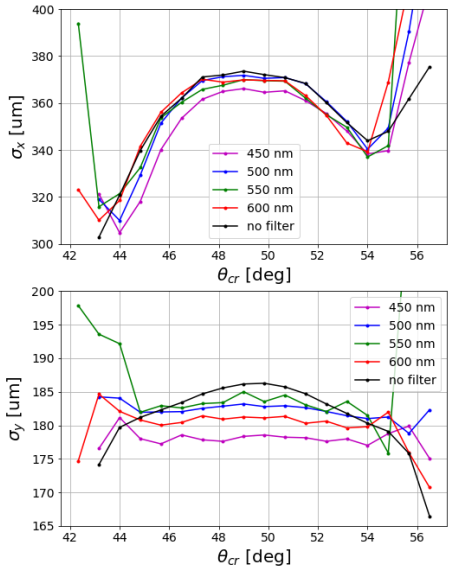

Figure 5: Sizes comparison with 0.6 mm thick crystal and different bandpass filters inserted.

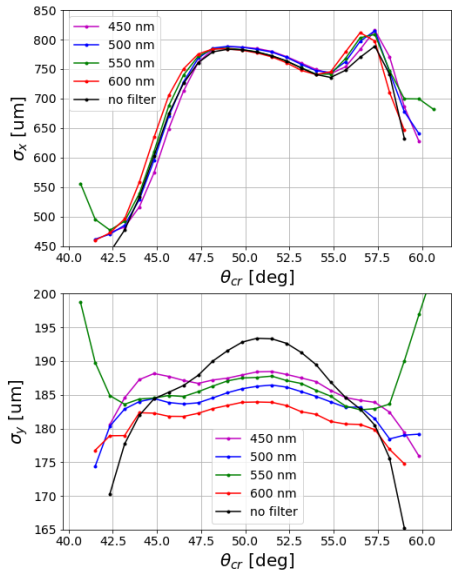

Figure 6: Sizes comparison with 2 mm thick crystal and different bandpass filters inserted.

peak intensities at lower angles, 53° and 54°, respectively. Additionally, a noticeable rise in the long-wavelength tail is observed for the 2 mm crystal.

The dependence of the total spectral intensity on the observation angle is shown in Fig. 8. All curves are normalized to their respective maximum values. The figure reveals a shift in the position of the maximum intensity as a function of crystal thickness. The 0.6 mm and 1 mm crystals behave similarly, differing by only about 1°, and coincide well in the range between 47° and 50°. In contrast, the 2 mm crystal exhibits a larger shift of approximately between 3° and 4°. This effect can be attributed to multiple scattering inside

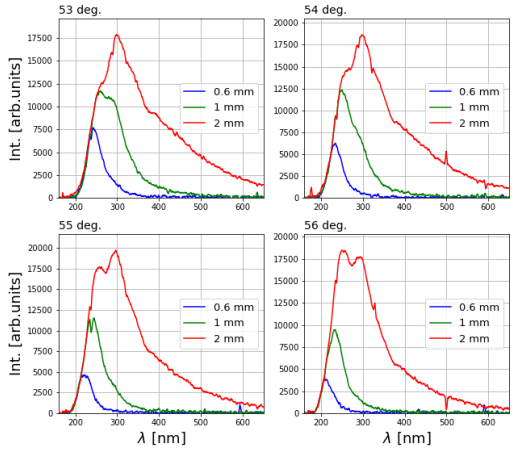

Figure 7: Spectra from 0.6, 1 and 2 mm crystals at 4 angles.

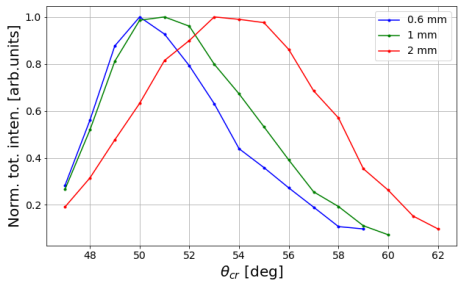

Figure 8: Total spectral intensity on angle for the three crystals.

the crystal, and in addition the beam traverses 60 mm of air before reaching the crystal. According to the work [9], the critical radiator thickness beyond which multiple scattering must be considered is given by

$$L_{cr} = 0.077\sqrt[3]{\lambda^2 X_0 \left(\frac{\gamma}{\sin\theta_{ch}}\right)}, \quad (3)$$

where X_0 is the radiation length. In our case the X_0 = 122.9 mm, then, substituting the other parameters into the equation, one gets 140 µm for λ = 550 nm. That can possibly even explain the difference between the 0.6 and 1 mm crystals. However further investigations are needed to prove it.

CONCLUSION

The measurements presented in this work compare five fused silica crystals of different thicknesses with a GAGG:Ce scintillator. Under certain conditions - specifically, for vertical sizes with bandpass filters applied - the crystal measurements appeared smaller. In addition, spectral measurements were performed, which may have indicated an influence of multiple scattering. Both of these aspects, however, require further investigation.

ISBN: 978-3-95450-262-2 ISSN: 2673-5350 doi: 10.18429/JACoW-IBIC2025-TUPCO22

REFERENCES

[1] B.M. Bolotovskii, "Vavilov-Cherenkov radiation: its discovery and application", *Phys.–Usp.*, vol. 52, pp. 1099–1110, 2009. doi:10.3367/UFNe.0179.200911c.1161

[2] J.D. Jackson, *Classical Electrodynamics*, UC Berkeley, NY, USA: John Wiley and Sons, 1998.

[3] D.E. Andersson *et al.*,"Lead fluoride: an ultra-relativistic Cherenkov radiator for EM calorymetry", *Nucl. Instrum. Methods*, vol. 290, pp. 385-389, May 1990. doi:10.1016/0168-9002(90)90553-I

[4] S.V. Schelkunov *et al.*, "Nondestructive diagnostic for electron bunch length in accelerators using the wakefield radiation spectrum", *Phys. Rev. Spec. Top. Accel. Beams*, vol. 8, p. 062801, Jun. 2005. doi:10.1103/PhysRevSTAB.8.062801

[5] A.M. Cook *et al.*, "Observation of narrow-band terahertz coherent Cherenkov radiation from a cylindrical dielectric-lined waveguide", *Phys. Rev. Lett.*, vol. 103, p. 095003, Aug. 2009. doi:10.1103/PhysRevLett.103.095003

[6] T. Lefevre *et al.*, "Cherenkov Diffraction Radiation as a tool for beam diagnostics", in *Proc. IBIC'19*, Malmö, Sweden, Sep. 2019, pp. 660–664. doi:10.18429/JACoW-IBIC2019-THAO01

[7] S. Wesch *et al.*, "Observation of Coherent Optical Transition Radiation and Evidence for Microbunching in Magnetic Chicanes", in *Proc. FEL'09*, Liverpool, UK, Aug. 2009, paper WEPC50, pp. 619–622.

[8] A. I. Novokshonov *et al.*, "Scintillator Nonproportionality Studies at PITZ", in *Proc. IBIC'22*, Kraków, Poland, Sep. 2022, pp. 277–280. doi:10.18429/JACoW-IBIC2022-TUP21

[9] B. Durnic *et al.*, "Radiator thickness and its effects on Cherenkov spectral lines", *Nucl. Instrum. Methods*, vol. 1059, p. 169015, Feb. 2024. doi:10.1016/j.nima.2023.169015